2025, 65(12): 5294-5308
CSTR: 32112.14.j.AMS.20250245
DOI: 10.13343/j.cnki.wsxb.20250245

微生物学报
Acta Microbiologica Sinica
http://journals.im.ac.cn/actamicrocn

Research Article 研究报告

脱叶链霉菌中白菖烯合酶基因的鉴定

高彦微[1]，张梦倩[1]，陈珂[1]，李静[1,2]，刘道占[1]，蔡由生[1]，邓子新[1]，朱冬青[1*]

1 武汉大学 药学院，组合生物合成与新药发现教育部重点实验室，湖北 武汉
2 广州医科大学附属第三医院，生物医学研究中心，广东 广州

高彦微, 张梦倩, 陈珂, 李静, 刘道占, 蔡由生, 邓子新, 朱冬青. 脱叶链霉菌中白菖烯合酶基因的鉴定[J]. 微生物学报, 2025, 65(12): 5294-5308.
GAO Yanwei, ZHANG Mengqian, CHEN Ke, LI Jing, LIU Daozhan, CAI Yousheng, DENG Zixin, ZHU Dongqing. Identification of a calarene synthase gene from *Streptomyces exfoliatus*[J]. Acta Microbiologica Sinica, 2025, 65(12): 5294-5308.

摘　要：【目的】确认脱叶链霉菌 UC5319 中法尼烯焦磷酸(farnesyl diphosphate, FPP)环化酶基因 *orf2064* 的功能。【方法】采用大肠杆菌蛋白表达系统对 *orf2064* 进行表达，纯化重组蛋白，以 FPP 为底物开展体外反应，利用气相色谱质谱仪(GC-MS)检测产物。构建可高效合成 FPP 的大肠杆菌基因工程菌，对 *orf2064* 进行异源表达，通过 GC-MS 检测发酵产物，并从发酵产物中分离纯化目标产物，利用核磁共振(nuclear magnetic resonance spectroscopy, NMR)确定其结构。以链霉菌为宿主对 *orf2064* 进行异源表达，用 GC-MS 检测发酵产物。【结果】ORF2064 重组蛋白体外反应产物、*orf2064* 大肠杆菌异源表达产物和链霉菌异源表达产物在 GC-MS 分析中均显示产生了 1 种保留时间相同、分子量为 204 的产物，分离纯化后经 NMR 分析确认其为白菖烯。【结论】脱叶链霉菌中基因 *orf2064* 所编码的 FPP 环化酶为白菖烯合酶。

关键词：白菖烯合酶；倍半萜；链霉菌

资助项目：国家重点研发计划(2021YFA0909500)；国家自然科学基金(81373305, 31401057)
This work was supported by the National Key Research and Development Program of China (2021YFA0909500) and the National Natural Science Foundation of China (81373305, 31401057).
*Corresponding author. Tel: +86-27-68759996, E-mail: Dzhu2011@whu.edu.cn
ORCID: ZHU Dongqing (0000-0002-6298-512X)
Received: 2025-03-26; Accepted: 2025-05-22; Published online: 2025-06-26

Identification of a calarene synthase gene from *Streptomyces exfoliatus*

GAO Yanwei[1], ZHANG Mengqian[1], CHEN Ke[1], LI Jing[1,2], LIU Daozhan[1], CAI Yousheng[1], DENG Zixin[1], ZHU Dongqing[1*]

1 Key Laboratory of Combinatorial Biosynthesis and Drug Discovery, Ministry of Education, School of Pharmaceutical Sciences, Wuhan University, Wuhan, Hubei, China

2 Biomedicine Research Center, the Third Affiliated Hospital of Guangzhou Medical University, Guangzhou, Guangdong, China

Abstract: [Objective] To confirm the function of the farnesyl diphosphate (FPP) cyclase encoded by *orf2064* in *Streptomyces exfoliatus* UC5319. **[Methods]** *orf2064* was expressed in *Escherichia coli*, and the recombinant protein was purified and assayed with FPP as the substrate. The reaction products were detected by GC-MS. An FPP-overproducing *E. coli* strain was engineered for heterologous expression of *orf2064*. The fermentation products were analyzed by GC-MS, and the target compound was isolated and structurally characterized by nuclear magnetic resonance spectroscopy (NMR). In addition, *orf2064* was heterologously expressed in *Streptomyces*, and the fermentation products were analyzed by GC-MS. **[Results]** GC-MS revealed that both the *in vitro* reaction of the recombinant protein ORF2064 and the heterologous expression products in *E. coli* and *Streptomyces* consistently produced a compound with identical retention time and $[M^+]$ of *m*/*z* 204. Subsequent isolation, purification, and NMR analysis confirmed this compound as calarene. **[Conclusion]** The FPP cyclase encoded by *orf2064* in *S. exfoliatus* is identified as an calarene synthase.

Keywords: calarene synthase; sesquiterpene; *Streptomyces*

Sesquiterpenes are a family of natural products with a variety of biological activities that are widely distributed in microbes and plants[1-5]. Calarene (**2**) and its derivatives are sesquiterpenes typically found in plants, including those used in traditional Chinese medicine or as spices, such as *Nardostachys* spp.[6-10], *Schisandra chinensis*[11], *Kadsura heteroclite*[12], *Aquilaria* spp.[13], *Panax* spp.[14-16], *Acorus* spp.[17-18], *Piper cordoncillo*[19], *Valeriana* spp.[20-21], *Humulus lupulus*[22], *Trichosanthes kirilowii*[23], and *Patrinia scabiosaefolia*[24].

Calarene appears effective against the larvae of the malaria vector *Anopheles stephensi*, the dengue vector *Aedes aegypti*, and the filariasis vector *Culex* spp.[12]. Calarene was also shown to have a sedative effect[13]. Calarene derivatives kanshone C and nardosinone are proven serotonin transporter (SERT) inhibitors[7]. However, some calarene derivatives have the property of SERT activators, including 1(10)-aristolen-9β-ol, kanshone H, nardostachone, nardochalaristolones C, and nardoflavaristolone A[7,25]. SERT is a classic drug target for neuropsychiatric and digestive disorders. The study of active molecules acting on SERT could contribute to drug discovery for mood disorders such as depression, anxiety, or obsessive-compulsive disorder, and for digestive disorders such as irritable bowel syndrome, slow transit constipation, and functional abdominal bloating[7]. Nardosinone and kanshone B, the peroxide

derivatives of calarene, inhibit NF-κB- and MAPK-mediated inflammatory pathways, demonstrating their potential in the treatment of neuroinflammation[26].

Although certain sesquiterpene synthases produce calarene in trace amounts as a byproduct, no genuine calarene synthase has been identified to date. Here, we focused on a putative terpene synthase gene *orf2064* in *Streptomyces exfoliatus* UC5319. Biochemical assays and heterologous expressions in this work proved that *orf2064* is a calarene synthase gene.

1 Materials and methods

1.1 Main reagents

Reagents and solvents were purchased and were of the highest quality available, and were used without further purification. Restriction enzymes, T4 DNA ligase, and DNA polymerase were obtained from New England Biolabs and Beijing Tsingke Biotech Co., Ltd., and were used according to the manufacturer's specifications. Ni-NTA affinity columns were sourced from GE Healthcare and Beyotime Biotech Co., Ltd., Shanghai, China. Amicon Ultra Centrifugal Filters were acquired from Millipore. DNA primers were synthesized by Beijing Tsingke Biotech Co., Ltd. and Sangon Biotech (Shanghai) Co., Ltd..

1.2 Strain culture conditions and product detection methods

The growth media and conditions for *Escherichia coli* and *Streptomyces* strains, as well as the standard methods for handling the strains, were previously described. *Bacillus subtilis* was cultivated in SR medium (25 g/L yeast extract, 15 g/L tryptone, 3 g/L K_2HPO_4, pH 7.2) at 37 ℃. *Enterococcus faecium*, *Enterococcus faecalis*, and *Streptococcus pneumoniae* were cultivated in TSYE medium (30 g/L trypticase soy broth, 3 g/L yeast extract) at 37 ℃. *Pantoea ananatis* was cultivated in TSB medium (30 g/L trypticase soy broth) at 30 ℃. DNA sequencing was performed by Tsingke Biotech Co., Ltd. or Sangon Biotech (Shanghai) Co., Ltd. Protein concentrations were determined using the Bradford method with bovine serum albumin as the standard. Protein purity was assessed by SDS-PAGE. An Agilent 7890A/5975C-GC/MSD at 70 eV electron impact (positive ion mode) and an HP5MS capillary column (30 m× 0.25 mm, 0.25 μm) were used for the GC-MS analysis of the terpenes. The conditions were as follows: a solvent delay of 3 min, a temperature program starting at 60 ℃ for 2 min, a temperature gradient from 60−280 ℃ for 11 min at 20 ℃/min, and a hold at 280 ℃ for 2 min. Samples were also analyzed using HPLC (Shimadzu SPD-M20A/LC-20AT) with a ThermoFisher Scientific C18 reversed-phase HPLC column (250 mm×4.6 mm, 5 μm). The HPLC conditions for terpenes (mobile phase A: water; mobile phase B: acetonitrile; UV detection λ: 210 nm) were as follows: 80% B for 30 min at a flow rate of 0.8 mL/min. The HPLC conditions for lycopene (mobile phase A: methanol; mobile phase B: acetonitrile; UV detection λ: 471 nm) were as follows: 30% B for 30 min at a flow rate of 1.0 mL/min.

1.3 Expression and purification of recombinant ORF2064 protein

A 1 044 bp DNA fragment containing *orf2064* was inserted into *Nde* I and *Not* I sites of pET28a to generate plasmid pCK11. *E. coli* BL21(DE3) harboring the plasmid pCK11 was cultured with LB medium containing 50 μg/mL kanamycin at 37 ℃. IPTG (isopropyl β-D-1-thiogalactopyranoside) was added to a final concentration of 0.1 mmol/L when the OD_{600} of the culture reached 0.6−0.8. The culture was further incubated at 18 ℃ overnight and centrifuged at 5 000×*g* for 15 min. The cells were harvested and resuspended in lysis buffer (300 mmol/L NaCl, 50 mmol/L Tris-HCl, 10 mmol/L imidazole, pH 7.4). The cells were disrupted by sonication and then centrifuged at 20 000×*g* for 60 min. The supernatant was transferred to a Ni-NTA column. The column was washed with wash buffer (20 mmol/L imidazole in lysis buffer). Protein was eluted with elution buffer (200 mmol/L imidazole in lysis buffer). Fractions were analyzed

by SDS-PAGE. The purified recombinant ORF2064 protein was concentrated and buffer-exchanged into storage buffer (PBS buffer, pH 7.4, containing 10% glycerol) using an Amicon Ultra centrifugal filter (10 kDa MWCO).

1.4 Incubation of recombinant ORF2064 with farnesyl diphosphate

Purified recombinant protein ORF2064 (1 μmol/L) was incubated with 20 μmol/L FPP in 1 mL of assay buffer (50 mmol/L PIPES, 100 mmol/L NaCl, 15 mmol/L $MgSO_4$, 5 mmol/L β-mercaptoethanol, 20% glycerol, pH 6.8) overlaid with 1 mL of *n*-hexane at 30 ℃ for 16 h. The reaction mixture was quenched with 25 μL of 500 mmol/L EDTA and extracted three times with *n*-hexane. The organic extracts were dried over anhydrous Na_2SO_4, concentrated, and analyzed by GC-MS.

1.5 Construction of the plasmids harboring lycopene biosynthetic genes, MEP pathway genes or MVA pathway genes

The bacterial strains and plasmids utilized in this study have had their relevant data deposited in the National Microbiology Data Center (NMDC) under accession number NMDCX0002140. The primer sequences are also available under this same NMDC accession number.

pACYCDuet-1 and pCDFDuet-1 were used to construct the plasmids. To avoid burdening the *E. coli* host with too much protein expression, one of the T7 promoters of pACYCDuet-1 was replaced by the P_{tac} with a weaker transcriptional level to generate a new vector named pLJ74. Then the remaining T7 promoter of pLJ74 was also replaced by the P_{tac} to generate a new vector named pQQ21. One of the T7 promoters of pCDFDuet-1 was replaced by the P_{tac} to generate a new vector named pLJ81. Then the remaining T7 promoters of pLJ81 were replaced by the P_{tac} to generate a new vector named pLJ83.

DNA fragments harboring geranylgeranyl diphosphate synthase gene *crtE*, 15-*cis*-phytoene synthase gene *crtB*, and phytoene desaturase gene *crtI* were cloned from *P. ananatis* CGMCC 1.15633 and sequenced. According to the sequences, new primer pairs were synthesized to amplify *crtE*, ribosome binding site (RBS)-*crtB*, and RBS-*crtI*, respectively, which were inserted downstream of P_{tac} of pQQ21 successively to generate plasmid pQQ26.

DNA fragments harboring type II isopentenyl-diphosphate delta-isomerase gene *idi*, 1-deoxy-D-xylulose-5-phosphate synthase gene *dxs*, and polyprenyl synthetase gene *ispA* were cloned from *B. subtilis* R-179 and sequenced. New primer pairs were synthesized according to the sequences to amplify *idi*, RBS-*dxs*, and RBS-*ispA*, respectively, which were inserted downstream of P_{tac} of pLJ74 successively to generate plasmid pLJ79. The DNA fragment harboring P_{tac}, *idi*, *dxs*, and *ispA* from pLJ79 was also inserted into the corresponding sites of pQQ26 harboring *crtE-crtB-crtI* to generate plasmid pQQ27.

DNA fragments harboring hydroxymethylglutaryl-CoA reductase gene *mvaE*, hydroxymethylglutaryl-CoA synthase gene *mvaS*, mevalonate kinase gene *mvaK1*, diphosphomevalonate decarboxylase gene *mvaD*, phosphomevalonate kinase gene *mvaK2* and type II isopentenyl-diphosphate delta-isomerase *idi* were cloned from *Enterococcus faecium* R-026 and sequenced. The *mvaE*, RBS-*mvaS*, *mvaK1*, RBS-*mvaD*, RBS-*mvaK2*, and RBS-*idi* were amplified respectively, which were inserted in the downstream of two *tac* promoters of pLJ83 successively to generate plasmid pLJ91. DNA fragments harboring *mvaE* and *mvaS* were cloned from *Enterococcus faecalis* FA2-2 and sequenced. DNA fragments harboring *mvaK1*, *mvaD*, *mvaK2*, and *idi* were cloned from *Streptococcus pneumoniae* CGMCC 1.8722 and sequenced. Then the primer pairs were synthetized according to the sequences. Gene *mvaE* and RBS-*mvaS* were amplified and inserted downstream of one *tac* promoter of pLJ83, and gene *mvaK1*, RBS-*mvaD*, RBS-*mvaK2*, and RBS-*idi* were amplified and inserted downstream of another *tac* promoter to generate plasmid pYW7. Finally, RBS-*ispA* was amplified and inserted

downstream of *mvaS* of pYW7 to generate plasmid pYW14.

1.6 Fermentation, extraction, and quantitative analysis of lycopene

E. coli strains carrying the *crtE-crtB-crtI* plasmids were cultured in LB medium with antibiotics at 37 ℃ overnight. Then 1% (*V*/*V*) of the culture was transferred to 50 mL of fresh 2×YT medium (1% yeast extract, 1.6% tryptone, 0.5% NaCl, pH 7.0) and cultured at 37 ℃. IPTG was added to a final concentration of 0.1 mmol/L when the OD_{600} reached 0.4−0.6. The culture was further incubated at 28 ℃ for 24 h. Cells were harvested, freeze-dried, resuspended in acetone, and then disrupted by sonication. Cell debris was removed by centrifugation at 20 000×*g* for 5 min. The supernatant was filtered through a microporous membrane (0.22 μm, nylon) and used for HPLC analysis. The presence of lycopene in the samples was confirmed by the comparison of retention time and mass spectra with the pure authentic lycopene standard. The production of lycopene was measured using the external standard method.

1.7 Fermentation and product analysis of *E. coli* strains harboring *orf2064*

The *orf2064* gene was inserted into pET21a to generate plasmid pCK10. *E. coli* strains carrying pCK10 were cultured overnight at 37 ℃ in LB media with antibiotics. Then, 1% (*V*/*V*) of the culture was transferred to fresh 2×YT media and incubated at 37 ℃ until the OD_{600} reached 0.4−0.6. IPTG was added to a final concentration of 0.1 mmol/L, and the culture was further incubated at 28 ℃ for 3−4 h. The culture was then overlaid with *n*-hexane at 30 ℃ for overnight and extracted three times with *n*-hexane. The combined organic extracts were dried over anhydrous Na_2SO_4 and concentrated for GC-MS analysis. To obtain the target compound, the crude extract of approximately 250 mg from the 5 L culture was dissolved using *n*-hexane, preliminarily separated by using SiO_2 column chromatography, and further purified by HPLC. HPLC (Shimadzu SPD-M20A/LC-20AT) and ThermoFisher Scientific C18 reversed-phase HPLC column (250 mm×9.6 mm, 5 μm) were used in purification. The HPLC conditions (mobile phase A: water; mobile phase B: acetonitrile; UV detection λ: 210 nm) were as follows: 80% B for 30 min at a flow rate of 3 mL/min. 4 mg of the target compound was recovered and analyzed by NMR. Carbon-13 and proton spectra were recorded on a Bruker AVANCE 400 MHz NMR spectrometer operating at 400 MHz and 100 MHz for ^{1}H and ^{13}C respectively, equipped with a 5 mm BBFO Smart Probe. All experiments were carried out at 303 K in $CDCl_3$. The chemical shifts were reported in ppm and referenced to the solvent resonance signal ($CDCl_3$: ^{1}H δ_{ppm} 7.26, ^{13}C δ_{ppm} 77.16).

1.8 Fermentation and product analysis of *Streptomyces* strains harboring *orf2064*

The *orf2064* gene was inserted downstream of *ermE*p* of pIB139 to generate plasmid pCK12. *Streptomyces* strains carrying pCK12 were cultured overnight at 28 ℃ in TSBY medium (0.5% yeast extract, 3% tryptic soy broth, 10.3% sucrose) containing 50 μg/mL aparmycin. Then, 1% (*V*/*V*) of the culture was transferred to the fresh SFM medium (2% soy flour and 2% mannitol) and incubated at 28 ℃ for 7 days. The culture was then extracted three times with *n*-hexane. The organic extracts were dried over anhydrous Na_2SO_4 and concentrated for GC-MS analysis.

2 Results and discussion

2.1 Terpene biosynthetic gene cluster *orf2064−2065* of *S. exfoliatus*

Pentalenolactone (**3**) is the first typical sesquiterpene studied in detail[27-28]. The pentalenene synthase gene *penA* (GenBank accession number ADO85594.1) from *S. exfoliatus* UC5319 encodes a 38 kDa monomer consisting of a single domain with a class I α-helical terpene cyclase fold and contains the conserved Asp-rich (DDXXD) and NSE/DTE motifs for binding the diphosphate moiety of the substrate along with three Mg^{2+}[28-30]. Pentalenene synthase catalyzes the cyclization of

FPP to pentalenene (**4**) (Figure 1A) [30-31]. Pentalenene (**4**) undergoes multi-step oxidoreductase catalysis to yield the final product, pentalenolactone (**3**)[32-36].

To find new terpene synthase genes, the genome of the pentalenolactone-producing strain *S. exfoliatus* UC5319 was scanned. We found a gene cluster containing two open reading frames, *orf2064* and *orf2065* (GenBank accession number PQ468278). Gene *orf2064* (Figure 2A, red arrow) encodes a 347 aa terpene synthase family protein with 22% identity and 37% similarity to

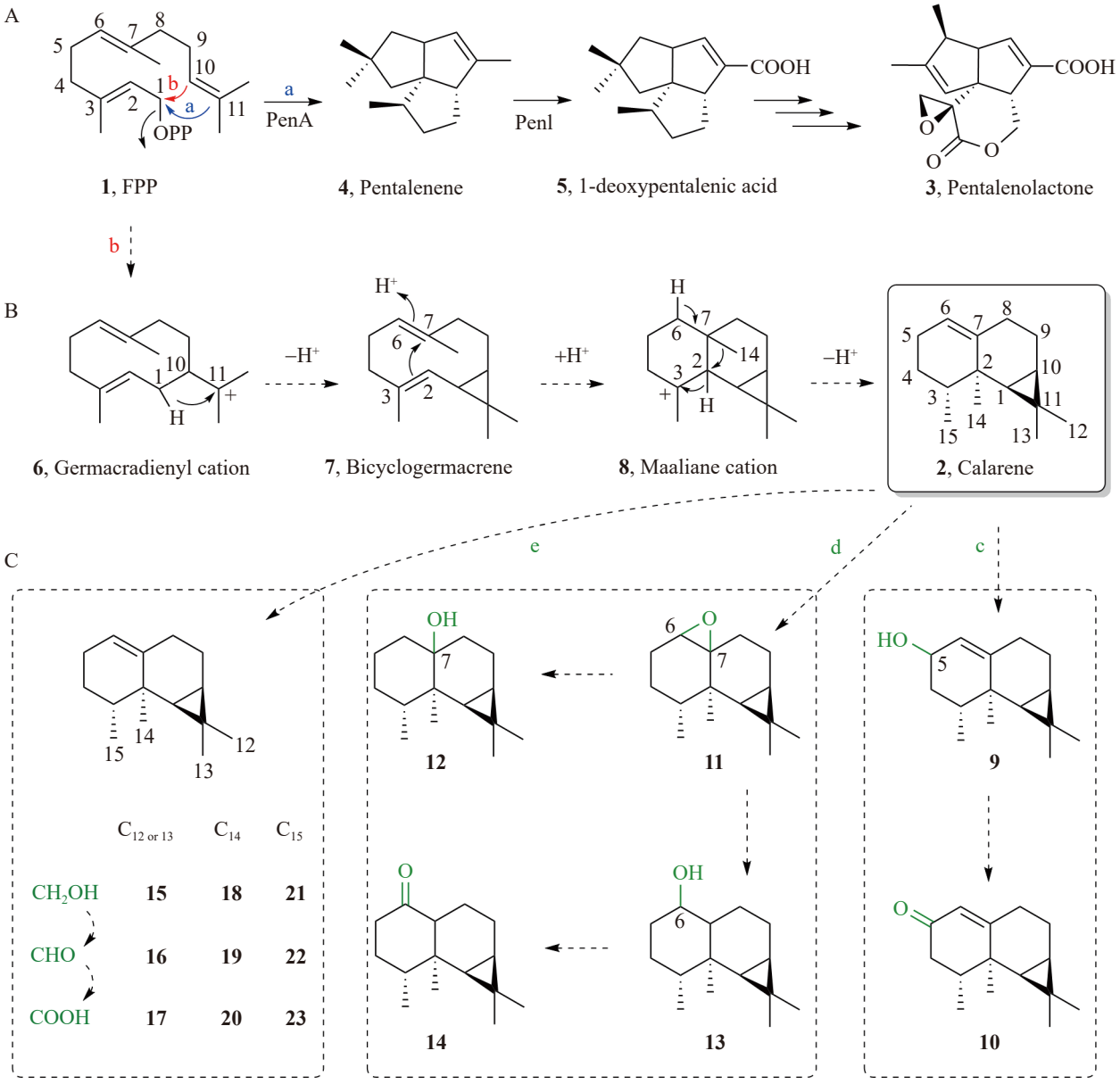

Figure 1 Biosynthetic pathway of pentalenolactone and proposed biosynthetic mechanism of calarene and derivatives of calarene. A: Biosynthetic pathway of pentalenolactone in *Streptomyces exfoliatus* UC5319[27-28]; B: Proposed biosynthetic mechanism of calarene; C: Proposed biosynthetic mechanism of derivatives of calarene.

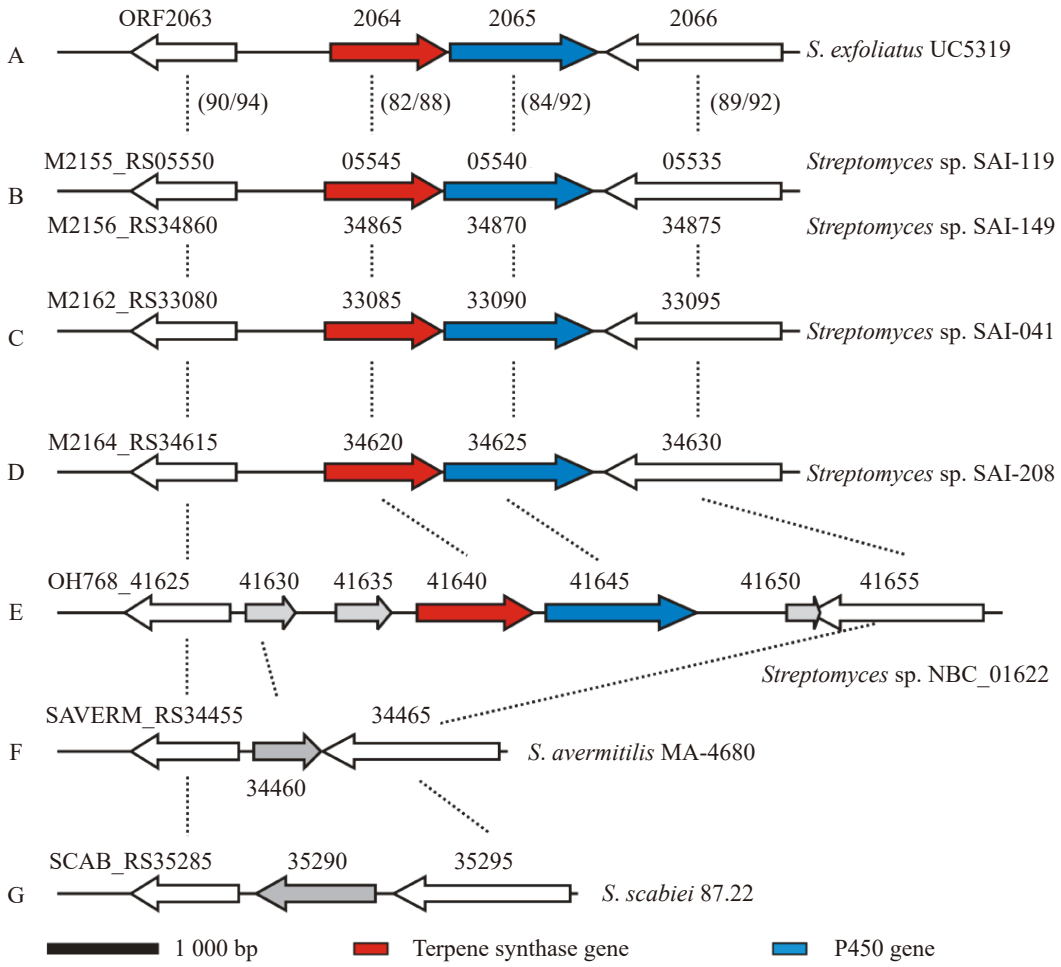

Figure 2 Terpene biosynthetic gene clusters in *Streptomyces*. A: *orf2064*−*orf2065* gene cluster in *S. exfoliatus* UC5319 (GenBank accession number PQ468278.1); B: Homologous gene clusters in *Streptomyces* sp. SAI-119 (NCBI reference sequence: NZ_JARXYH010000001.1) and SAI-149 (NZ_JARXYI010000001.1); C: *Streptomyces* sp. SAI-041 (NZ_JARXYO010000001.1); D: *Streptomyces* sp. SAI-208 (NZ_JARXYQ010000002.1); E: *Streptomyces* sp. NBC_01622 (NZ_CP109293.1); F: The homologous genes of *orf2063* and *orf2066* in *S. avermitilis* MA-4680 (NC_003155.5); G: *S. scabiei* 87.22 (NC_013929.1). The numbers in brackets show the percent of sequence identity and similarity at the protein level with corresponding genes in the *S. exfoliatus* UC5319.

pentalenene synthase PenA. ORF2064 displays the two highly conserved Mg^{2+}-binding motifs of terpene synthases, the aspartate-rich ^{109}DDGVCD motif and the downstream ^{251}NDLFSYLKE motif. Similar to all other terpene synthases, the conserved motifs are separated by 142 amino acids. Gene *orf2065* (Figure 2A, blue arrow) downstream of *orf2064* encodes a 441 aa cytochrome P450 monooxygenase with 41% identity and 57% similarity to PenI (GenBank accession number ADO85595.1), which catalyzes the oxidative conversion of pentalenene (**4**) to 1-deoxypentalenic acid (**5**) (Figure 1A). The upstream gene *orf2063* encodes a RluA family pseudouridine synthase, and the downstream gene *orf2066* encodes a putative amino acid permease.

Homologs of the gene *orf2063*−*orf2066* are present in some *Streptomyces* spp. strains (Figure 2B−2E). However, the homologs of *orf2064* and *orf2065* are replaced by a GNAT family N-acetyltransferase gene SAVERM_RS34460 in *S. avermitilis* MA-4680 (Figure 2F) and a terpene cyclase gene SCAB_RS35290 of unknown function (with 24% identity and 37% similarity to ORF2064 at the amino acid level) in *S. scabiei* 87.22 (Figure 2G) between the homologs of *orf2063* and *orf2066*.

2.2 Biochemical characterization of recombinant ORF2064

To identify the function of ORF2064, gene *orf2064* was amplified and inserted into the *E. coli* expression vector pET28a to generate plasmid pCK11. pCK11 was transferred into *E. coli* BL21(DE3) to express recombinant ORF2064. The recombinant ORF2064 protein was purified by Ni-NTA chromatography (Figure 3A). The purified recombinant ORF2064 protein was incubated with

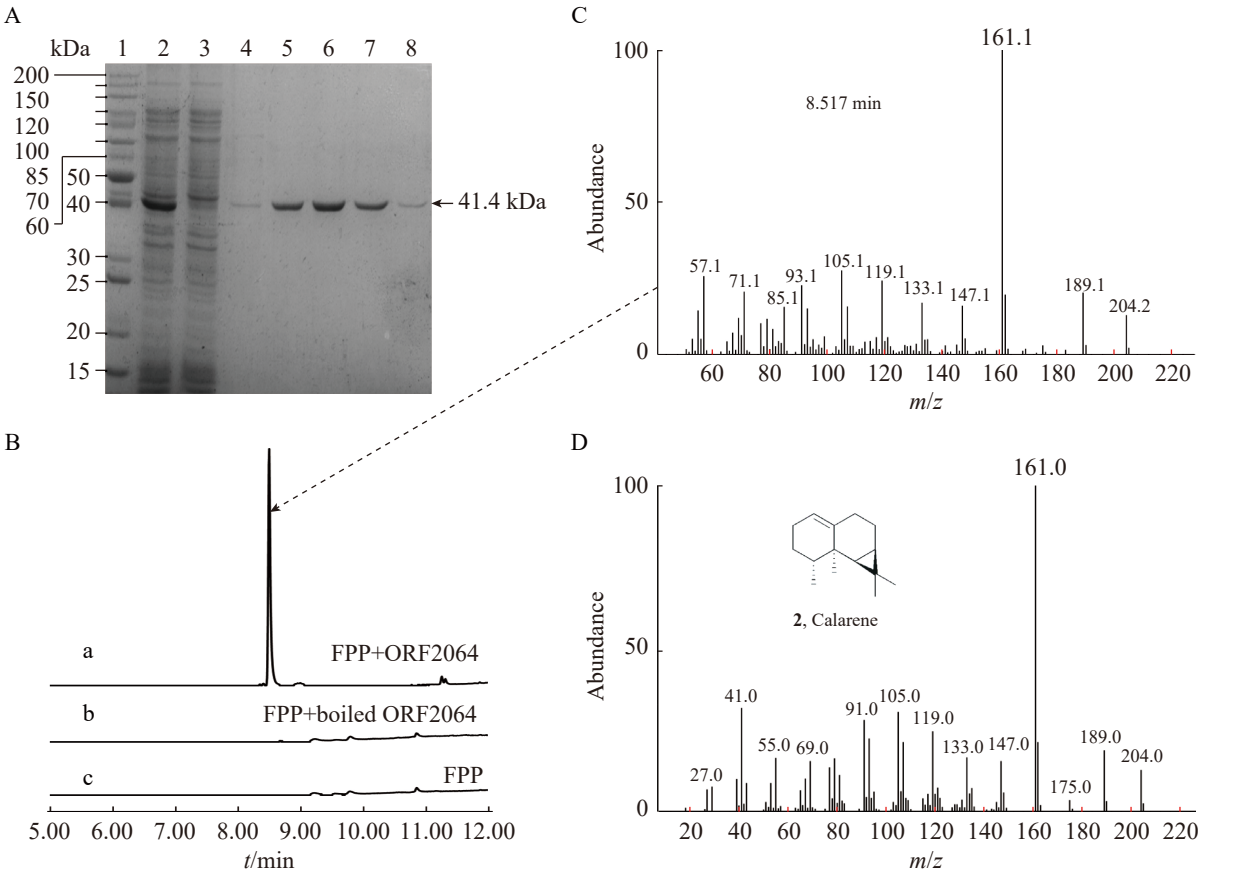

Figure 3 GC-MS analysis of incubations of recombinant ORF2064 protein with FPP. A: SDS-PAGE analysis of purified recombinant ORF2064 protein (Lane 1: Protein marker; Lane 2: Supernatant after sonication; Lane 3: Flow-through of supernatant after binding with Ni^{2+} resin; Lane 4: Flow-through of Ni^{2+} resin washed with 50 mmol/L imidazole; Lane 5 to Lane 8: Elution containing 100, 150, 200 and 250 imidazole, respectively); B: GC-MS analysis of incubations of purified recombinant ORF2064 protein with FPP (a: The incubation of FPP with recombinant ORF2064 protein; b: Control incubation of FPP with boiled recombinant ORF2064 protein; c: Control standard FPP); C: Mass spectrum of the peak of retention time 8.517 min; D: Mass spectrum of calarene from the library of the National Institute of Standards and Technology.

20 μmol/L FPP in the presence of 15 mmol/L Mg^{2+} at 30 ℃ for 16 h. The mixture was quenched with EDTA and then extracted with *n*-hexane. The organic extracts were dried, concentrated, and tested by using GC-MS. GC-MS analysis showed the formation of a single sesquiterpene with an [M^+] of *m/z* 204 and a base peak of 161.1 (Figure 3B, 3C). Comparison of the spectrum in the National Institute of Standards and Technology MS database allowed us to identify the compound as calarene (**2**) (Figure 3D).

2.3 Engineered *E. coli* host for the efficient *in vivo* synthesis of terpenes

The pure authentic standard of calarene could not be purchased; therefore, the product of FPP catalyzed by ORF2064 had to be isolated and purified for structural identification. To obtain sufficient quantities of the target compound, we used an engineered *E. coli* host BL21(DE3) (pMH1, pFZ81) designed for the efficient *in vivo* synthesis of terpenoid metabolites[37]. Gene *orf2064* was inserted into pET21a to generate plasmid pCK10, which was transferred into *E. coli* BL21(DE3) (pMH1, pFZ81). The GC-MS analysis revealed a sesquiterpene with an [M^+] of *m/z* 204 (not shown), consistent with the product of FPP cyclization catalyzed by recombinant ORF2064 protein *in vitro*. According to GC-MS analysis, the production in this work was lower than 0.05 mg/L. A host cell with higher FPP production was therefore needed.

We need a reporter system to compare the FPP production of engineered *E. coli* hosts intuitively. FPP is the precursor for lycopene biosynthesis, so the red tetraterpenoid lycopene was chosen as a reporter. The plasmid pQQ26 was constructed (Figure 4A), carrying three lycopene biosynthesis genes amplified from *Pantoea ananatis* (geranylgeranyl diphosphate synthase gene *crtE*, 15-*cis*-phytoene synthase gene *crtB*, and phytoene desaturase gene *crtI*, GenBank accession numbers were PQ468284 and PQ468285). The resulting strain *E. coli* BL21(DE3) (pQQ26) turned a pale red, indicating that the reporter system was working.

Next, the plasmids pYW7, pYW14, pYW13, and pLJ91, which carry the genes of the mevalonate (MVA) pathway from different sources, were constructed separately. Plasmid pYW7 (Figure 4A) was constructed using MVA genes amplified from *Enterococcus faecalis* (hydroxymethylglutaryl-CoA reductase gene *mvaE* and hydroxymethylglutaryl-CoA synthase gene *mvaS*, GenBank accession number PQ468287 and PQ468286) and *Streptococcus pneumoniae* (mevalonate kinase gene *mvaK1*, diphosphomevalonate decarboxylase gene *mvaD*, phosphomevalonate kinase gene *mvaK2*, and type 2 isopentenyl-diphosphate delta-isomerase gene *idi*, GenBank accession number PQ468288). Gene *ispA* from *B. subtilis* (GenBank accession number PQ468280) was inserted into pYW7 to generate the plasmid pYW14 (Figure 4A). pYW13 is derived from a plasmid pJBEI-6410[38] carrying MVA genes, a GPP synthase gene, and a limonene synthase gene from different sources. The GPP synthase gene of pJEBI-6410 was replaced with the FPP synthase gene *ispA* amplified from *B. subtilis*, and the limonene synthase gene of pJEBI-6410 was deleted to generate plasmid pYW13. Plasmid pLJ91 contains MVA genes and *ispA* amplified from *Enterococcus faecium* (GenBank accession numbers were PQ468281, PQ468282, and PQ468283).

The plasmids were separately transferred into *E. coli* BL21(DE3) (pQQ26) and the resulting transformants were cultured and induced with IPTG. BL21(DE3) (pQQ26, pYW7) and BL21(DE3) (pQQ26, pYW14) showed deeper red comparing with the control strain BL21(DE3) (pQQ26, pLJ83). BL21(DE3) (pQQ26, pLJ91) and BL21(DE3) (pQQ26, pYW13) didn't deepen (not shown). HPLC and the pure authentic standard of lycopene were used to analyze the production of lycopene (Figure 4B, 4C). The result showed that the lycopene production of the control strain BL21(DE3) (pQQ26, pLJ83) was 0.09 mg/L in this work and that the lycopene production of BL21(DE3) (pQQ26, pYW7) increased 42-fold (about 3.93 mg/L) (Figure 4C, red columns). The lycopene production of BL21(DE3) (pQQ26, pYW14) (about 4.26 mg/L)

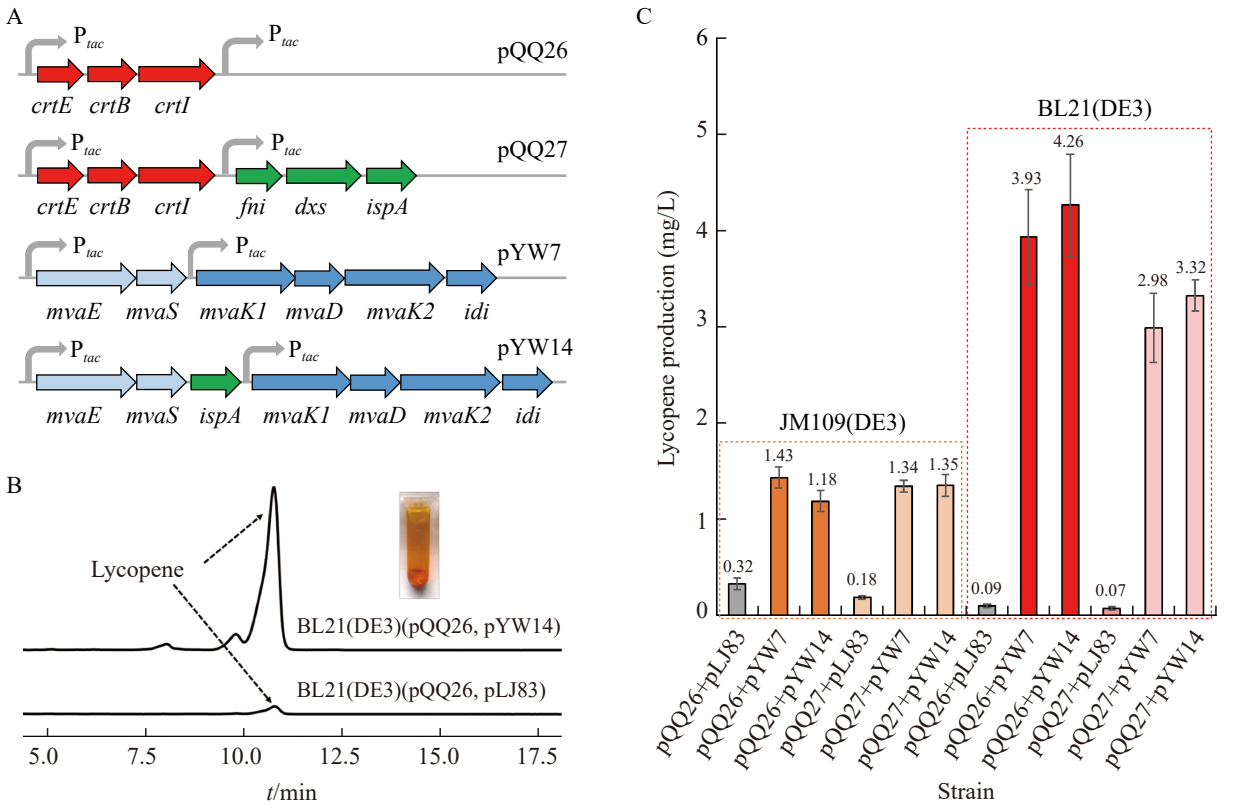

Figure 4 Construction of *Escherichia coli* host for the efficient *in vivo* synthesis of terpenes. A: Schematic representation of some key plasmids (Red arrows: Genes from *P. ananatis*; Green arrows: Genes from *B. subtilis*; Light blue arrows: Genes from *Enterococcus faecalis*; Deep blue arrows: Genes from *Streptococcus pneumoniae*); B: HPLC analysis of *E. coli* strain BL21(DE3) (pQQ26, pYW14) and control strain *E. coli* BL21(DE3) (pQQ26, pLJ83) [pLJ83: The vector of pYW7 and pYW14; The tube: The extraction of BL21(DE3) (pQQ26, pYW14) cells]; C: Lycopene production of *E. coli* strains detected and quantified by HPLC [Gray columns: Negative controls; Orange columns and light orange columns: *E. coli* JM109(DE3) strains; Red columns and light red columns: *E. coli* BL21(DE3) strains; Error bars indicate the standard deviation (n=3)].

didn't increase significantly compared to BL21(DE3) (pQQ26, pYW7).

In summary, we constructed an *E. coli* host BL21(DE3) (pYW7) for the efficient *in vivo* synthesis of terpenes, which can be used to obtain sufficient quantities of the sesquiterpene product in the next work.

2.4 Heterologous expression of *orf2064* in *E. coli* BL21(DE3) (pYW7)

The plasmid pCK10 carrying *orf2064* was transformed into *E. coli* BL21(DE3) (pYW7). The GC-MS analysis of the culture of BL21(DE3) (pYW7, pCK10) gave a main product with the same characteristics as the product of ORF2064-catalyzed cyclization of FPP (Figure 5A, 5B). The culture containing the target compound was isolated by using SiO_2 column chromatography and semi-preparative HPLC, and tested by using GC-MS (NMDCX0002140). The target compound purified was analyzed by NMR (NMDCX0002140): ^{13}C NMR (100 MHz, $CDCl_3$) δ 144.3, 120.5, 36.9, 36.8, 33.6, 30.0, 29.9, 27.4, 25.9, 23.1, 21.0, 19.7,

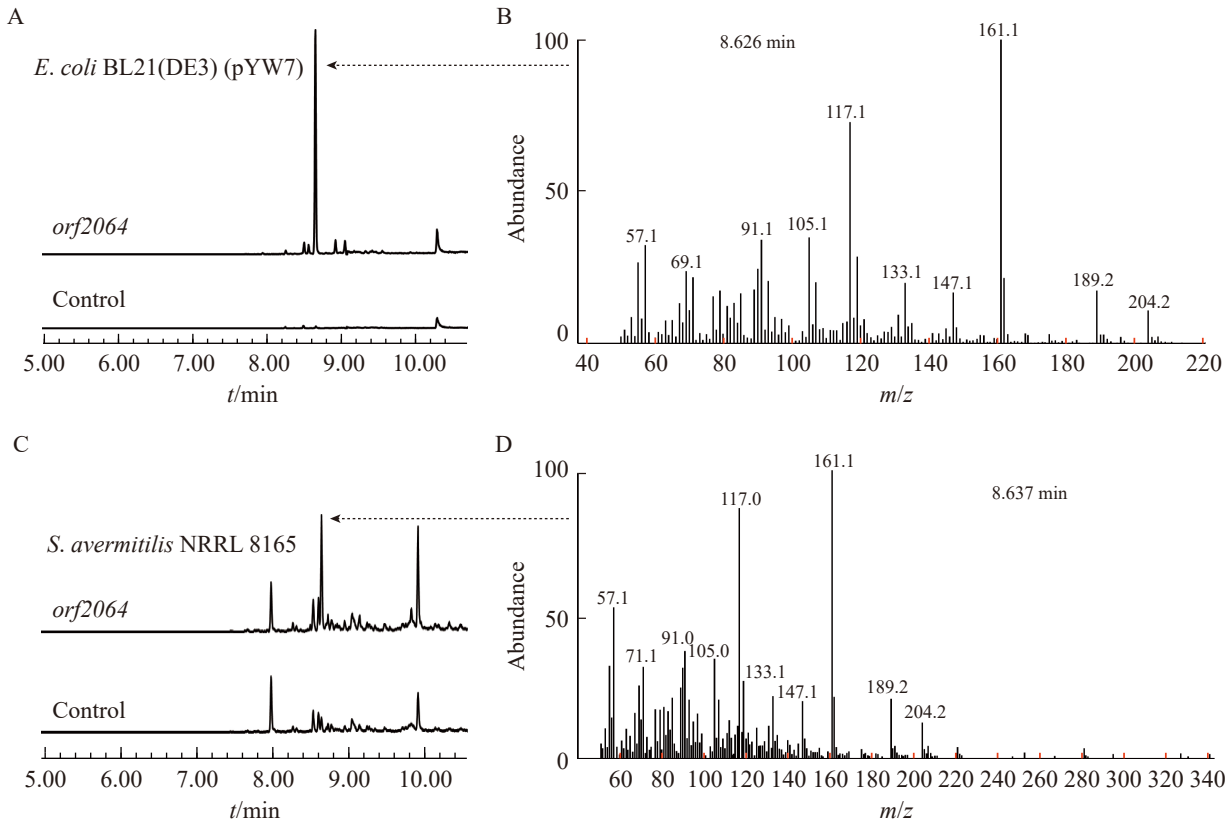

Figure 5 GC-MS analysis of heterologous expression experiments of *orf2064*. A: *E. coli* BL21(DE3) as host [*orf2064*: *E. coli* BL21(DE3) (pCK10, pYW7); Control: *E. coli* BL21(DE3) (pET21a, pYW7)]; B: Mass spectrum of the peak of retention time 8.626 min; C: *S. avermitils* NRRL 8165 as host (*orf2064*: *S. avermitils* NRRL 8165::pCK12; Control: *S. avermitils* NRRL 8165::pIB139); D: Mass spectrum of the peak of retention time 8.637 min.

18.7, 16.7, 16.2 ppm; ^{1}H NMR (400 MHz, $CDCl_3$) δ 5.24 (m, 1H), 2.23 (m, 1H), 1.99−1.92 (m, 3H), 1.76 (m, 1H), 1.73 (m, 1H), 1.42 (m, 2H), 1.39 (m, 1H), 1.07 (s, 3H), 1.02 (s, 3H), 0.97 (d, J=7.7 Hz, 6H), 0.74 (m, 1H), 0.56 (d, J=9.2 Hz, 1H). The results showed that ^{1}H and ^{13}C NMR spectra of the compound were consistent with the published NMR spectra of calarene[6] (NMDCX0002140). In summary, *in vivo* heterologous expression of *orf2064* in *E coli* showed that ORF2064 is a calarene synthase.

2.5 Heterologous expression of *orf2064* in *Streptomyces*

Several media were used to culture *S. exfoliatus* UC5319 and no calarene or its derivatives were found (data not shown). Gene cluster *orf2064−2065* may be silent in *S. exfoliatus* UC5319. *S. avermitilis* was selected to express *orf2064*. Gene *orf2064* was inserted into the *Streptomyces* expression vector pIB139 to generate plasmid pCK12. pCK12 was transferred into *S. avermitilis* NRRL 8165. The resultant strain *S. avermitilis* NRRL 8165::pCK12 was cultured. GC-MS analysis showed a sesquiterpene product with the same characteristics as the product of the *E. coli* strain harboring *orf2064* (Figure 5C, 5D). In summary, *in vivo* heterologous expression of *orf2064* in *Streptomyces* showed that ORF2064 is a calarene synthase.

3 Discussion

3.1 Proposed biosynthetic mechanism of calarene

Sesquiterpenes are generated from FPP, and their structural diversity results from the first step catalyzed by sesquiterpene synthases. Sesquiterpene synthases convert FPP and generate and control the reactivity of high-energy carbenium ion intermediates in reactions involving carbon skeleton rearrangement, and methyl and hydride migration[31,39-40]. According to other sesquiterpene synthase cyclization mechanisms[28,31,41-43], we presumed that the cyclization mechanism catalyzed by calarene synthase is initiated by ionization of the allylic diphosphate ester to the corresponding allylic cation-pyrophosphate ion pair, and subsequent electrophilic attack at C10 of the distal double bond, resulting in the formation of the intermediate germacradienyl cation (**6**) (Figure 1B). Insertion of the 2-propyl cation into the C−H bond with loss of the original proton would result in the formation of bicyclogermacrene (**7**). The intermediate bicyclogermacrene (**7**) would be further cyclized by protonation at C6 and intramolecular attack of the resulting carbocation on the C-2, 3 bond to form the maaliane cation (**8**). Subsequent methyl migration and hydride shift, followed by deprotonation of C6, would then lead to the formation of calarene. The exact mechanism of cyclization needs to be investigated in future work.

3.2 Cytochrome P450 monooxygenase gene *orf2065*

We also focused on the cytochrome P450 monooxygenase gene *orf2065*. According to the structure of calarene, we presumed three possible oxidations catalyzed by ORF2065 (Figure 1C). First, ORF2065 may catalyze the conversion of C5 to the compound 10 (also known as 1(10)-aristolen-2-one) by stepwise oxidation *via* the compound 9. Second, ORF2065 may catalyze the epoxidation of the C6−C7 double bond to the compound 11, followed by the ring-opening reaction to produce the compound 12, or the compounds 13 and 14. Third, ORF2065 may catalyze the carboxylation of C12 (C13, C14, or C15) to the compound 17 (or 20, 23) by stepwise oxidation *via* the compound 15 (or 18, 21) and 16 (or 19, 22).

To confirm the function of the ORF2065 protein, *orf2065* was amplified and inserted into pET28a to generate plasmid pCK14, which was transferred into *E. coli* BL21(DE3) to express. However, soluble recombinant protein of ORF2065 was not obtained. We tried feeding assays in *E. coli* BL21(DE3) (pCK14) by using calarene as the substrate. GC-MS analysis of the organic extract of the cultures. We wanted to find the new peak with an $[M^+]$ of *m/z* 220 (the compound 9, 11, 14, 15, 18, or 21), 218 (the compound 10, 16, 19, or 22), or 222 (the compound 12 or 13). While we didn't find any new peaks. The organic extract was also methylated with TMS-CHN_2 and analyzed by GC-MS. The new peak with an $[M^+]$ of *m/z* 248 (methyl esters of the compound 17, 20, or 24) was not observed. Typical bacterial P450s require electron transport proteins for catalysis. We presumed that there are no auxiliary proteins (the ferredoxin reductase and ferredoxin) of ORF2065 in *E. coli* so *Streptomyces* may be a better host for ORF2065 expression. The *orf2064* and *orf2065* genes were amplified and inserted into pIB139 to generate plasmid pCK17, which was transferred into *S. avermitilis* NRRL 8165. NRRL 8165:: pCK17 was cultured. GC-MS analysis of the organic extract. No new peak with an $[M^+]$ of *m/z* 220, 218, 222, or 248 was observed.

A BLASTp search of the NCBI protein database with the ORF2065 sequence revealed 11 sequence records of *Streptomyces* proteins with high degrees of sequence similarity and identity. Sequence alignment of ORF2065 and its homologs revealed that ORF2065 has 10 residues that differ from those at homologous sites found in its homologs, including Y37, R120, L135, T203, C267, R274, A330, S405, A409, and the absence of a glutamic acid residue between A376 and R377 (NMDCX0002140). We speculate that a mutation in one or more of the key residues may have

rendered ORF2065 inactive.

3.3 *E. coli* host for the efficient *in vivo* synthesis of terpenes

An efficient host for FPP biosynthesis is useful in functional studies of sesquiterpene synthase. Here, we constructed *E. coli* BL21(DE3) (pYW7) for the efficient *in vivo* synthesis of terpenes. Unlike pJEBI-6410, pMH1, and pFZ81 carrying MVA genes from *Saccharomyces cerevisiae* and *E. coli*, pYW7 with a higher plasmid copy number and stronger promoters contains MVA genes from *Streptococcus pneumoniae* and *Enterococcus faecalis*. These differences may have contributed to pYW7 being more effective in this study.

To further enhance the production, the gene *ispA* and two key enzyme genes of the methylerythritol 4-phosphate (MEP) pathway in *B. subtilis* including type II isopentenyl-diphosphate delta-isomerase gene *idi* (GenBank accession number PQ468279) and 1-deoxy-D-xylulose-5-phosphate synthase gene *dxs* (GenBank accession number PQ468280), were inserted into pQQ26 to generate plasmid pQQ27, which was transferred into BL21(DE3) (pYW7), BL21(DE3) (pYW14) and the control strain BL21(DE3) (pLJ83). HPLC analysis showed that the lycopene production of the strains containing pQQ27 decreased by 22%−24% compared to the strains containing pQQ26, which was unexpected (Figure 4C, pink columns).

E. coli JM109(DE3) was also used in this study. The results showed that lycopene production of JM109(DE3) strains decreased by 55%−72% compared to BL21(DE3) strains (Figure 4C, orange columns and light orange columns).

4 Conclusion

We cloned a terpene synthase gene *orf2064* from *S. exfoliatus* UC5319. Incubation of purified recombinant protein ORF2064 with FPP in the presence of Mg^{2+} generated a sesquiterpene product. An engineered *E. coli* host BL21(DE3) (pYW7) was constructed for the efficient *in vivo* synthesis of FPP. Gene *orf2064* was transferred into BL21 (DE3) (pYW7) for heterologous expression, and the same product was observed. NMR analysis of the isolated product identified the sesquiterpene as calarene. Heterologous expression of *orf2064* using *S. avermitilis* NRRL 8165 as the host also yielded the product calarene. The calarene synthase identified in this study provided a valuable tool for the biosynthesis of active compounds with a calarene skeleton.

Credit authorship contribution statement

GAO Yanwei: Investigation, Writing-original draft; ZHANG Mengqian: Investigation, Methodology; CHEN Ke: Investigation; LI Jing: Writing-original draft; LIU Daozhan: Methodology; CAI Yousheng: Supervision; DENG Zixin: Resources; ZHU Dongqing: Conceptualization, Funding acquisition, Writing-review & editing.

Declaration of competing interest

The authors declare no competing financial interest.

References

[1] LUO P, HUANG JH, LV JM, WANG GQ, HU D, GAO H. Biosynthesis of fungal terpenoids[J]. Natural Product Reports, 2024, 41(5): 748-783.
[2] MA MY, LI MK, WU ZK, LIANG XQ, ZHENG QS, LI DF, WANG GL, AN TY. The microbial biosynthesis of noncanonical terpenoids[J]. Applied Microbiology and Biotechnology, 2024, 108(1): 226.
[3] DEWICK PM. The biosynthesis of C5 − C25 terpenoid compounds[J]. Natural Product Reports, 2002, 19(2): 181-222.
[4] FRAGA BM. Natural sesquiterpenoids[J]. Natural Product Reports, 2005, 22(4): 465-486.
[5] CANE DE. Enzymic formation of sesquiterpenes[J]. Chemical Reviews, 1990, 90(7): 1089-1103.
[6] FURUSAWA M, HASHIMOTO T, NOMA Y, ASAKAWAA Y. Biotransformation of aristolane- and 2,3-secoaromadendrane-type sesquiterpenoids having a 1,1-dimethylcyclopropane ring by *Chlorella fusca* var. *vacuolata*, *Mucor* species, and *Aspergillus niger*[J]. Chemical & Pharmaceutical Bulletin, 2006, 54(6): 861-868.
[7] CHEN YP, YING SS, ZHENG HH, LIU YT, WANG ZP, ZHANG H, DENG X, WU YJ, GAO XM, LI TX, ZHU Y, XU YT, WU HH. Novel serotonin transporter regulators: natural aristolane- and nardosinane-types of sesquiterpenoids from *Nardostachys chinensis* Batal[J].

Scientific Reports, 2017, 7: 15114.
[8] TANAKA K, KOMATSU K. Comparative study on volatile components of *Nardostachys* rhizome[J]. Journal of Natural Medicines, 2008, 62(1): 112-116.
[9] SATYAL P, CHHETRI BK, DOSOKY NS, POUDEL A, SETZER WN. Chemical composition of *Nardostachys* grandiflora rhizome oil from Nepal: a contribution to the chemotaxonomy and bioactivity of *Nardostachys*[J]. Natural Product Communications, 2015, 10(6): 1067-1070.
[10] WANG JH, ZHAO JL, LIU H, ZHOU LG, LIU ZL, WANG JG, HAN JG, YU Z, YANG FY. Chemical analysis and biological activity of the essential oils of two valerianaceous species from China: *Nardostachys chinensis* and *Valeriana officinalis*[J]. Molecules, 2010, 15(9): 6411-6422.
[11] LEE HJ, CHO IH, LEE KE, KIM YS. The compositions of volatiles and aroma-active compounds in dried omija fruits (*Schisandra chinensis* Baillon) according to the cultivation areas[J]. Journal of Agricultural and Food Chemistry, 2011, 59(15): 8338-8346.
[12] GOVINDARAJAN M, RAJESWARY M, BENELLI G. δ-cadinene, calarene and. δ-4-carene from kadsura *Heteroclita* essential oil as novel larvicides against malaria, dengue and filariasis mosquitoes[J]. Combinatorial Chemistry & High Throughput Screening, 2016, 19(7): 565-571.
[13] TAKEMOTO H, ITO M, SHIRAKI T, YAGURA T, HONDA G. Sedative effects of vapor inhalation of agarwood oil and spikenard extract and identification of their active components[J]. Journal of Natural Medicines, 2008, 62(1): 41-46.
[14] CHEN SY, RUI R, WANG S, HE XH. Comparative analysis of the floral fragrance compounds of *Panax notoginseng* flowers under the *Panax notoginseng-pinus* agroforestry system using SPME-GC-MS[J]. Molecules, 2022, 27(11): 3565.
[15] LEE SJ, MOON TW, LEE J. Increases of 2-furanmethanol and maltol in Korean red ginseng during explosive puffing process[J]. Journal of Food Science, 2010, 75(2): C147-C151.
[16] CHO IH, LEE HJ, KIM YS. Differences in the volatile compositions of ginseng species (*Panax* sp.)[J]. Journal of Agricultural and Food Chemistry, 2012, 60(31): 7616-7622.
[17] YAN L, LIU ZZ, XU L, QIAN YY, SONG PP, WEI M. Identification of volatile active components in *Acori Tatarinowii* Rhizome essential oil from different regions in China by C6 glioma cells[J]. BMC Complementary Medicine and Therapies, 2020, 20(1): 255.
[18] BERTEA CM, AZZOLIN CMM, BOSSI S, DOGLIA G, MAFFEI ME. Identification of an *Eco*R I restriction site for a rapid and precise determination of β-asarone-free *Acorus calamus* cytotypes[J]. Phytochemistry, 2005, 66(5): 507-514.
[19] ALONSO-HERNÁNDEZ N, GRANADOS-ECHEGOYEN C, VERA-REYES I, PÉREZ-PACHECO R, ARROYO-BALÁN F, VALDEZ-CALDERÓN A, ESPINOSA-ROA A, LOEZA-CONCHA HJ, VILLANUEVA-SÁNCHEZ E, GARCÍA-PÉREZ F, DIEGO-NAVA F. Assessing the larvicidal properties of endemic campeche, Mexico plant *Piper cordoncillo* var. *apazoteanum* (Piperaceae) against *Aedes aegypti* (Diptera: Culicidae) mosquitoes[J]. Insects, 2023, 14(4): 312.
[20] RAINA AP, NEGI KS. Essential oil composition of *Valeriana jatamansi* Jones from Himalayan regions of India[J]. Indian Journal of Pharmaceutical Sciences, 2015, 77(2): 218-222.
[21] TAHERPOUR AA, MAROOFI H, BAJELANI O, LARIJANI K. Chemical composition of the essential oil of *Valeriana alliariifolia* Adams of Iran[J]. Natural Product Research, 2010, 24(10): 973-978.
[22] Van OPSTAELE F, PRAET T, AERTS G, de COOMAN L. Characterization of novel single-variety oxygenated sesquiterpenoid hop oil fractions *via* headspace solid-phase microextraction and gas chromatography-mass spectrometry/olfactometry[J]. Journal of Agricultural and Food Chemistry, 2013, 61(44): 10555-10564.
[23] WU SM, XU T, AKOH CC. Effect of roasting on the volatile constituents of *Trichosanthes kirilowii* seeds[J]. Journal of Food and Drug Analysis, 2014, 22(3): 310-317.
[24] LIN J, CAI QY, XU W, LIN JM, PENG J. Chemical composition, anticancer, anti-neuroinflammatory, and antioxidant activities of the essential oil of *Patrinia scabiosaefolia*[J]. Chinese Journal of Integrative Medicine, 2018, 24(3): 207-212.
[25] DENG X, WANG Y, WU HH, ZHANG WZ, DONG XQ, WANG ZM, ZHU Y, GAO XM, LI L, WANG YN, XU YT, Six kanshone C-derived sesquiterpenoid hybrids nardochalaristolones A−D, nardoflavaristolone A and dinardokanshone F from *Nardostachys jatamansi* DC[J]. Bioorganic Chemistry, 2018, 81: 35-43
[26] KO W, PARK JS, KIM KW, KIM J, KIM YC, OH H. Nardosinone-type sesquiterpenes from the hexane fraction of *Nardostachys jatamansi* attenuate NF-κB and MAPK signaling pathways in lipopolysaccharide-stimulated BV2 microglial cells[J]. Inflammation, 2018, 41(4): 1215-1228.
[27] QUADERER R, OMURA S, IKEDA H, CANE DE. Pentalenolactone biosynthesis. molecular cloning and assignment of biochemical function to PtlI, a cytochrome P450 of *Streptomyces avermitilis*[J]. Journal of the American Chemical Society, 2006, 128(40): 13036-13037.
[28] LESBURG CA, ZHAI G, CANE DE, CHRISTIANSON DW. Crystal structure of pentalenene synthase: mechanistic insights on terpenoid cyclization reactions in biology[J]. Science, 1997, 277(5333): 1820-1824.
[29] CANE DE, PARGELLIS C. Partial purification and characterization of pentalenene synthase[J]. Archives of Biochemistry and Biophysics, 1987, 254(2): 421-429.
[30] CANE DE, SOHNG JK, LAMBERSON CR, RUDNICKI

SM, WU Z, LLOYD MD, OLIVER JS, HUBBARD BR. Pentalenene synthase. purification, molecular cloning, sequencing, and high-level expression in *Escherichia coli* of a terpenoid cyclase from *Streptomyces* UC5319[J]. Biochemistry, 1994, 33(19): 5846-5857.

[31] MATOS JO, KUMAR RP, MA AC, PATTERSON M, KRAUSS IJ, OPRIAN DD. Mechanism underlying anti-Markovnikov addition in the reaction of pentalenene synthase[J]. Biochemistry, 2020, 59(35): 3271-3283.

[32] SEO MJ, ZHU DQ, ENDO S, IKEDA H, CANE DE. Genome mining in *Streptomyces*. elucidation of the role of baeyer-villiger monooxygenases and non-heme iron-dependent dehydrogenase/oxygenases in the final steps of the biosynthesis of pentalenolactone and neopentalenolactone[J]. Biochemistry, 2011, 50(10): 1739-1754.

[33] ZHU DQ, SEO MJ, IKEDA H, CANE DE. Genome mining in *Streptomyces*. discovery of an unprecedented P450-catalyzed oxidative rearrangement that is the final step in the biosynthesis of pentalenolactone[J]. Journal of the American Chemical Society, 2011, 133(7): 2128-2131.

[34] ZHU DQ, WANG YP, ZHANG MM, IKEDA H, DENG ZX, CANE DE. Product-mediated regulation of pentalenolactone biosynthesis in *Streptomyces* species by the MarR/SlyA family activators PenR and PntR[J]. Journal of Bacteriology, 2013, 195(6): 1255-1266.

[35] CHEN K, WU SW, ZHU L, ZHANG CD, XIANG WS, DENG ZX, IKEDA H, CANE DE, ZHU DQ. Substitution of a single amino acid reverses the regiospecificity of the baeyer-villiger monooxygenase PntE in the biosynthesis of the antibiotic pentalenolactone[J]. Biochemistry, 2016, 55(48): 6696-6704.

[36] DUAN L, JOGL G, CANE DE. The cytochrome P450-catalyzed oxidative rearrangement in the final step of pentalenolactone biosynthesis: substrate structure determines mechanism[J]. Journal of the American Chemical Society, 2016, 138(38): 12678-12689.

[37] ZHU FY, ZHONG XF, HU MZ, LU L, DENG ZX, LIU TG. *In vitro* reconstitution of mevalonate pathway and targeted engineering of farnesene overproduction in *Escherichia coli*[J]. Biotechnology and Bioengineering, 2014, 111(7): 1396-1405.

[38] ALONSO-GUTIERREZ J, CHAN R, BATTH TS, ADAMS PD, KEASLING JD, PETZOLD CJ, LEE TS. Metabolic engineering of *Escherichia coli* for limonene and perillyl alcohol production[J]. Metabolic Engineering, 2013, 19: 33-41.

[39] CANE DE, YANG GH, XUE Q, SHIM JH. Trichodiene synthase. substrate specificity and inhibition[J]. Biochemistry, 1995, 34(8): 2471-2479.

[40] CHRISTIANSON DW. Structural and chemical biology of terpenoid cyclases[J]. Chemical Reviews, 2017, 117(17): 11570-11648.

[41] JIANG JY, HE XF, CANE DE. Geosmin biosynthesis. *Streptomyces coelicolor* germacradienol/germacrene D synthase converts farnesyl diphosphate to geosmin[J]. Journal of the American Chemical Society, 2006, 128(25): 8128-8129.

[42] CHOU WKW, FANIZZA I, UCHIYAMA T, KOMATSU M, IKEDA H, CANE DE. Genome mining in *Streptomyces avermitilis*: cloning and characterization of SAV_{76}, the synthase for a new sesquiterpene, avermitilol[J]. Journal of the American Chemical Society, 2010, 132(26): 8850-8851.

[43] FELICETTI B, CANE DE. Aristolochene synthase: mechanistic analysis of active site residues by site-directed mutagenesis[J]. Journal of the American Chemical Society, 2004, 126(23): 7212-7221.